

## CHAPTER 8

Quantum Electrodynamics  
of One-Photon Wave PacketsM. Stobińska<sup>a</sup>, G. Alber<sup>b</sup> and G. Leuchs<sup>a</sup>

Contents	1. Introduction	201
	2. Quantum Electrodynamics of a Material Two-level System—Basic Aspects	203
	2.1. The Jaynes–Cummings–Paul model	203
	2.2. Spontaneous emission of a photon in free space	206
	3. Quantum Electrodynamics with Controlled Mode Selection	210
	3.1. Photon exchange in a closed spherical cavity	210
	3.2. Spontaneous photon emission in a half-open parabolic cavity	214
	4. Conclusions and Outlook	222
	References	224

## 1. INTRODUCTION

Excited bound states of atoms are one of the simplest examples of unstable quantum states which decay radiatively into the continuum of possible one-photon states of the electromagnetic field in free space. The search for a satisfactory theoretical explanation of the line frequencies and intensities of photon emission spectra at the beginning of the last century eventually culminated in Heisenberg's "magical paper" from July 1925 [1,2] and in the

<sup>a</sup> Max Planck Institute for the Science of Light - Günther-Scharowsky-Str.1, Bau 24, 91058 Erlangen, Germany

<sup>b</sup> Institut für Angewandte Physik, Technische Universität Darmstadt, Hochschulstraße 4a, 64289 Darmstadt, Germany

01 development of modern quantum mechanics [3–6]. Although basic aspects  
02 of this spontaneous decay process have already been described theoret-  
03 ically in an adequate way in the early days of modern quantum mechanics  
04 [7, 8], interestingly, some of its time-dependent dynamical aspects are still of  
05 topical current interest.

06 To a large part the current interest in this elementary photon emission  
07 process is due to recent advances in quantum technology. They have enabled  
08 one to prepare quantum states of matter and of the electromagnetic field to  
09 such a high level of precision that not only subtle quantum electrodynamical  
10 phenomena can be tested experimentally but that these phenomena can also  
11 be exploited practically for purposes of quantum information processing [9].  
12 On the one hand it is possible to engineer quantum states of individual  
13 atoms or even of multiparticle systems with the help of sophisticated par-  
14 ticle traps. In this context electromagnetic fields play a predominant role for  
15 achieving the required trapping and they also allow to control the material  
16 quantum states involved with an unprecedented level of accuracy [10, 11].  
17 On the other hand it is also possible to engineer quantum states of the elec-  
18 tromagnetic field. Not only classical electromagnetic fields with large photon  
19 numbers can be generated by sophisticated pulse shaping techniques [12]  
20 but also particular few-photon quantum states of the electromagnetic field  
21 can be prepared in a controlled way [13]. Numerous current developments  
22 in the area of quantum electrodynamics, for example, have emanated from  
23 an early insight of E.A. Purcell [14] that a modified density of field modes  
24 of the electromagnetic field influences spontaneous decay rates. This stimu-  
25 lated numerous experiments demonstrating the suppression of spontaneous  
26 decay in cavities [15, 16]. More recently it has even been demonstrated that  
27 extreme selection of electromagnetic field modes by cavities in combina-  
28 tion with trapping of single atoms enables one to control the interaction  
29 between single atoms and the electromagnetic field [13]. Thus, it is possible  
30 to prepare single-photon single-mode quantum states of the electromag-  
31 netic field [17], for example, or to excite a single atom by a single-photon  
32 quantum state perfectly with the help of vacuum Rabi oscillations [18].  
33 Despite these significant advances of quantum electrodynamics similar effi-  
34 cient techniques for preparing many-mode few-photon quantum states of  
35 the electromagnetic field or for controlling the resulting atom–field dynam-  
36 ics are significantly less well developed. Advances in this direction would  
37 be particularly interesting for purposes of quantum information process-  
38 ing. They would significantly enhance the flexibility of exchanging quantum  
39 information between the electromagnetic field, which is particularly useful  
40 for the transport of quantum information, and matter, which is well suited  
41 for the storage of quantum information.

42 In this contribution we investigate quantum electrodynamical many-mode  
43 aspects by exploring the simplest possible situation in this context, namely  
44 the interaction of a single atom, modeled by a simple two-level system,

01 with many-mode one-photon quantum states of the electromagnetic field  
 02 [19]. In particular, we concentrate on the question of how the engineer-  
 03 ing of electromagnetic field modes influences the atom–field interaction. An  
 04 interesting problem in this context is the engineering of ideal one-photon  
 05 multimode quantum states which may excite a single atom perfectly [20]. For  
 06 purposes of quantum information processing such one-photon multimode  
 07 states are particularly well suited for transmitting quantum information and  
 08 for storing it in a material memory again.

09 This chapter is organized as follows: In Section 2 characteristic aspects  
 10 of two extreme cases of the interaction of a simple two-state quantum  
 11 system with the radiation field are discussed, namely the single-mode  
 12 Jaynes–Cummings–Paul model [21, 22] and spontaneous photon emission  
 13 in free space [7, 8]. In Section 3 we explore dynamical modifications origi-  
 14 nating from modifications of the electromagnetic field modes involved. For  
 15 this purpose the interaction of a single photon with a two-level system in  
 16 a closed spherical cavity of arbitrary size [23] and in a half-open parabolic  
 17 cavity [24, 25] is explored.

18

19

## 20 **2. QUANTUM ELECTRODYNAMICS OF A MATERIAL TWO-LEVEL** 21 **SYSTEM—BASIC ASPECTS**

22

23 In this section basic results concerning the interaction of matter with the  
 24 quantized radiation field are discussed. For this purpose an elementary  
 25 two-level model of matter is considered which involves two nondegenerate  
 26 relevant energy eigenstates coupled almost resonantly to the electromagnetic  
 27 field. Characteristic quantum electrodynamical properties of this model sys-  
 28 tem are particularly apparent in cases in which the quantum states of the  
 29 electromagnetic field contain only a small number of photons. The resulting  
 30 dynamics depends significantly on whether only one mode of the radiation  
 31 field or an infinite number of them participate in the interaction.

32

### 33 **2.1. The Jaynes–Cummings–Paul model**

34

35 One of the simplest models which describes characteristic quantum features  
 36 of the almost resonant interaction of matter with the radiation field is the  
 37 Jaynes–Cummings–Paul model [21, 22]. In this model a material two-level  
 38 system interacts with a single mode of the radiation field. In the Schrödinger  
 39 picture its dynamics is described by the Hamiltonian

40

$$41 \hat{H} = E_g |g\rangle\langle g| + E_e |e\rangle\langle e| + \hbar\omega \hat{a}^\dagger \hat{a} + \hbar g \hat{a} |e\rangle\langle g| + \hbar g^* \hat{a}^\dagger |g\rangle\langle e|. \quad (1)$$

42

43 The energies of the material two-level system are denoted by  $E_g$  and  $E_e > E_g$   
 44 and  $\hat{a}$  ( $\hat{a}^\dagger$ ) is the destruction (creation) operator of the almost resonantly  
 coupled electromagnetic field mode of frequency  $\omega$ , i.e.,  $E_e - E_g \approx \hbar\omega$ .

The coupling constant  $g$  characterizes the strength of the interaction of the material two-level system with the single mode of the radiation field. In the dipole approximation, for example, which applies in typical quantum optical situations and in which it is assumed that the wavelength of the almost resonantly coupled electromagnetic field mode is significantly larger than the extension of the material charge distribution of the two-level system, this coupling constant is given by

$$\hbar g \hat{a} = -\langle e | \hat{\mathbf{d}} | g \rangle \cdot \hat{\mathbf{E}}_+(\mathbf{x}_0). \quad (2)$$

Thereby,  $\hat{\mathbf{d}}$  is the material dipole operator. The positive frequency component of the electric field operator is denoted by

$$\hat{\mathbf{E}}_+(\mathbf{x}) = i \sqrt{\frac{\hbar \omega}{2\epsilon_0}} \mathbf{u}(\mathbf{x}) \hat{a}, \quad (3)$$

and it has to fulfill the transversality condition  $\nabla \cdot \hat{\mathbf{E}}_+(\mathbf{x}) = 0$ . ( $\epsilon_0$  is the permittivity of vacuum.) The normalized mode function  $\mathbf{u}(\mathbf{x})$  is a solution of the Helmholtz equation

$$(\nabla^2 + \omega/c^2) \mathbf{u}(\mathbf{x}) = 0 \quad (4)$$

and fulfills the boundary conditions of the mode-selecting cavity involved. It is normalized according to the relation  $\int_{\mathbb{R}^3} d^3x |\mathbf{u}(\mathbf{x})|^2 = 1$ . The position of the center of mass of the material charge distribution is denoted by  $\mathbf{x}_0$ .

Within this model the dynamics of the almost resonantly coupled matter-field system can be described in a straightforward way by expanding the quantum state  $|\psi\rangle_t$  at time  $t$  in the basis of energy eigenstates of the uncoupled quantum system, i.e.,

$$|\psi\rangle_t = \sum_{n=0}^{\infty} \{a_{e,n}(t) e^{-i(E_e+n\hbar\omega)t/\hbar} |e\rangle \otimes |n\rangle + a_{g,n}(t) e^{-i(E_g+n\hbar\omega)t/\hbar} |g\rangle \otimes |n\rangle\}. \quad (5)$$

The time-dependent Schrödinger equation  $i\hbar d|\psi\rangle_t/dt = \hat{H}|\psi\rangle_t$  yields the system of pairs of coupled equations

$$\begin{aligned} \dot{a}_{e,n}(t) &= -ig\sqrt{n+1} e^{i\Delta t} a_{g,n+1}(t), \\ \dot{a}_{g,n+1}(t) &= -ig^* \sqrt{n+1} e^{-i\Delta t} a_{e,n}(t) \quad (\text{for } n \geq -1), \end{aligned} \quad (6)$$

with  $\Delta = (E_e - \hbar\omega - E_g)/\hbar$  denoting the detuning from resonance.

If initially, at  $t = 0$ , the two-level system is prepared in its excited state  $|e\rangle$ , i.e.,  $a_{g,n}(0) = 0$  for  $n \geq 0$ , Eqs. (6) yield the solution

$$\begin{aligned}
 a_{e,n}(t) &= a_{e,n}(0) \left( \cos\left(\frac{\Omega_n t}{2}\right) - \frac{i\Delta}{\Omega_n} \sin\left(\frac{\Omega_n t}{2}\right) \right) e^{i\Delta t/2}, \\
 a_{g,n+1}(t) &= -a_{e,n}(0) \frac{2ig^* \sqrt{n+1}}{\Omega_n} \sin\left(\frac{\Omega_n t}{2}\right) e^{-i\Delta t/2}.
 \end{aligned}
 \tag{7}$$

The time evolution of the probability amplitudes  $a_{e,n}(t)$  and  $a_{g,n}(t)$  exhibits a characteristic periodic energy transfer between the two-level system and the electromagnetic field mode which is characterized by the  $n$ -photon Rabi frequency  $\Omega_n = \sqrt{\Delta^2 + 4|g|^2(n+1)}$ . As the period of this energy exchange depends on the photon number the resulting time evolution exhibits interesting collapse and revival phenomena.

Let us consider a special case in more detail in which initially the two-level system is excited and the single-mode radiation field is in a coherent state  $|\alpha\rangle$  with  $\hat{a}|\alpha\rangle = \alpha|\alpha\rangle$  and  $\alpha \in \mathbb{C}$  [18]. The resulting time evolution of the inversion of the two-level system is given by

$$w(t) := \sum_{n=0}^{\infty} \{|a_{e,n}(t)|^2 - |a_{g,n}(t)|^2\} = \sum_{n=0}^{\infty} |a_{e,n}(0)|^2 \left( \frac{\Delta^2}{\Omega_n^2} + \frac{4|g|^2(n+1)}{\Omega_n^2} \cos(\Omega_n t) \right),
 \tag{8}$$

with  $a_{e,n}(0) = \exp(-|\alpha|^2/2)\alpha^n/\sqrt{n!}$ . In Figure (8.1) the time evolution of this inversion is depicted for resonant coupling, i.e.,  $\Delta = 0$ , and various values of the mean photon number  $\langle n \rangle = \langle \alpha | \hat{a}^\dagger \hat{a} | \alpha \rangle = |\alpha|^2$  of a coherent state  $|\alpha\rangle$ . It is apparent that the initially prepared inversion collapses after a characteristic collapse time of the order of  $T_c = 2\pi/|g|$ . Furthermore, at multiples of times of the order of  $T_r = 2\pi\sqrt{\langle n \rangle + 1}/|g|$  the probability amplitudes interfere constructively again thus causing revivals of the initial excitation [26, 27]. Finally, it should also be mentioned that according to Eq. (8) the appearance of collapse and revival phenomena does not necessarily require an initially prepared pure quantum state of the electromagnetic field.

If one considers the extreme case that the two-level system is excited initially but the electromagnetic field is in its ground (vacuum) state one obtains the result

$$w(t) = \frac{\Delta^2}{\Omega_0^2} + \frac{4|g|^2}{\Omega_0^2} \cos(\Omega_0 t)
 \tag{9}$$

for the inversion of the two-level system. In this case the inversion oscillates periodically between its extreme values and these oscillations are governed by the vacuum Rabi frequency  $\Omega_0 = 2|g|$ . In particular, this result demonstrates that in the case of the coupling of a two-level system to a single mode of the radiation field the decay of the excited state of the two-level

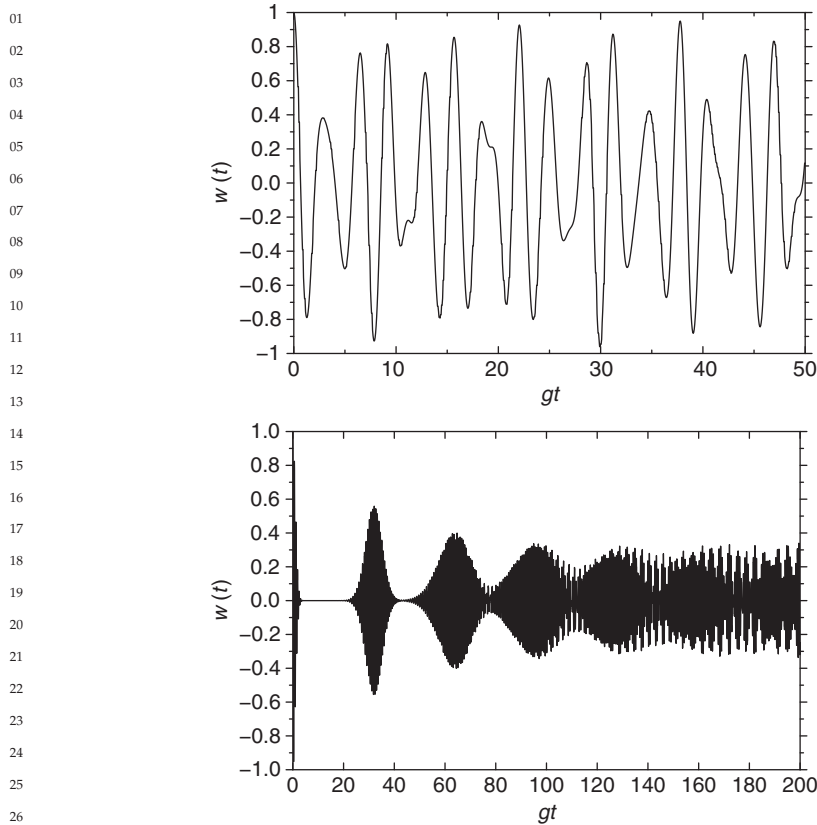


**Figure 8.1** Time dependence of the inversion  $w(t)$  of Eq. (8) of the two-level system describing its excitation by a coherent single-mode state  $|\alpha\rangle$ :  $\langle n \rangle = 0.5$  (left curve),  $\langle n \rangle = 25$  (right curve).

system is not described by an exponential decay law but exhibits a periodic energy exchange which reflects the periodic exchange of a photon between the two-level system and the radiation field.

## 2.2. Spontaneous emission of a photon in free space

If a material two-level system interacts with the quantized radiation field in free space its dynamics differs significantly from the single-mode case described previously. In order to exemplify these significant differences let us assume that initially the two-level system is prepared in its excited state  $|e\rangle$  and that the electromagnetic field is in its ground (vacuum) state  $|0\rangle$ . In the absence of any mode-selecting cavity all modes of the electromagnetic radiation field couple to this initially excited two-level system. In the Schrödinger

01 picture the field operators of the electric and magnetic field strengths are  
 02 given by [28]

$$03 \hat{\mathbf{E}}(\mathbf{x}) = \sum_{\mathbf{k},i} \sqrt{\frac{\hbar\omega_{\mathbf{k}}}{2\epsilon_0}} \{i\mathbf{u}_{\mathbf{k},i}(\mathbf{x})\hat{a}_{\mathbf{k},i} - i\mathbf{u}_{\mathbf{k},i}^*(\mathbf{x})\hat{a}_{\mathbf{k},i}^\dagger\} = \hat{\mathbf{E}}_+(\mathbf{x}) + \hat{\mathbf{E}}_-(\mathbf{x}), \quad (10)$$

$$04 \hat{\mathbf{B}}(\mathbf{x}) = \sum_{\mathbf{k},i} \sqrt{\frac{\hbar}{2\epsilon_0\omega_{\mathbf{k}}}} \{(\nabla \wedge \mathbf{u}_{\mathbf{k},i})(\mathbf{x})\hat{a}_{\mathbf{k},i} + (\nabla \wedge \mathbf{u}_{\mathbf{k},i}^*)(\mathbf{x})\hat{a}_{\mathbf{k},i}^\dagger\} = \hat{\mathbf{B}}_+(\mathbf{x}) + \hat{\mathbf{B}}_-(\mathbf{x}),$$

05 with their corresponding “positive-” and “negative-frequency” parts  $\hat{\mathbf{E}}_+(\mathbf{x})$   
 06 and  $\hat{\mathbf{E}}_-(\mathbf{x})$  ( $\hat{\mathbf{B}}_+(\mathbf{x})$  and  $\hat{\mathbf{B}}_-(\mathbf{x})$ ). If we consider an electromagnetic field in a cubic  
 07 quantization volume of length  $L$  and volume  $V = L^3$  and impose periodic  
 08 boundary conditions a complete set of orthonormal mode functions can be  
 09 chosen in the form

$$10 \mathbf{u}_{\mathbf{k},i}(\mathbf{x}) = \mathbf{e}_i(\mathbf{k}) \frac{e^{i\mathbf{k}\cdot\mathbf{x}}}{\sqrt{V}}, i = 1, 2, \quad (11)$$

11 with the wave vectors  $\mathbf{k} = 2\pi\mathbf{n}/L$  ( $\mathbf{n} \in \mathbb{Z}^3$ ) and with the corresponding real-  
 12 valued unit-polarization vectors  $\mathbf{e}_i(\mathbf{k})$  ( $\mathbf{e}_1(\mathbf{k}) \cdot \mathbf{e}_2(\mathbf{k}) = 0$ ,  $\mathbf{e}_1(\mathbf{k}) \wedge \mathbf{e}_2(\mathbf{k}) = \mathbf{k}/|\mathbf{k}|$ )  
 13 fulfilling the transversality condition  $\mathbf{e}_i(\mathbf{k}) \cdot \mathbf{k} = 0$  for  $i = 1, 2$ . Within a pertur-  
 14 bative treatment of the spontaneous photon emission process according to  
 15 Fermi’s golden rule the resulting decay of the two-level system is governed  
 16 by the rate [28]

$$17 \Gamma = \sum_{\mathbf{k},i} \frac{2\pi}{\hbar} |(e|\hat{\mathbf{d}}|g) \cdot \hat{\mathbf{E}}_+(\mathbf{x}_0)|^2 \delta(E_g + \hbar\omega_{\mathbf{k}} - E_e) = \frac{\omega_{eg}^3 |(e|\hat{\mathbf{d}}|g)|^2}{3\pi\epsilon_0\hbar c^3}, \quad (12)$$

18 with the transition frequency  $\omega_{eg} = \omega_{eg}$ . Within the framework of the dipole  
 19 approximation  $\mathbf{x}_0$  denotes the position of the center of mass of the two-level  
 20 system. It is apparent from Eq. (12) that the spontaneous decay rate depends  
 21 on the number of field modes per unit energy which couple resonantly, i.e.,  
 22 with  $\omega_{\mathbf{k}} = (E_e - E_g)/\hbar$ , to the spontaneously decaying two-level system. Thus,  
 23 altering the mode structure of these relevant field modes by a cavity, for  
 24 example, modifies the spontaneous decay rate. This effect was confirmed  
 25 in experiments with Rydberg atoms of sodium [29] excited in a niobium  
 26 superconducting cavity. Rydberg atoms are especially suitable for the exper-  
 27 imental verification of modifications of spontaneous decay rates since they  
 28 possess large dipole matrix elements on microwave transitions. Therefore,  
 29 the spontaneous emission rate for the atomic transition  $23S \rightarrow 22P$  was investi-  
 30 gated which was in resonance with the niobium superconducting cavity at

340 GHz. Thus, the free-space value of  $\Gamma = 150 \text{ s}^{-1}$  could be increased to a value of  $\Gamma_{\text{cavity}} = 8 \cdot 10^4 \text{ s}^{-1}$ .

A nonperturbative treatment of the exponential decay of an excited two-level system has already been given by Weisskopf and Wigner [7,8] in their seminal work. If the initially prepared quantum state of the matter–field system is of the form  $|e\rangle \otimes |0\rangle$  the time evolution of the resulting quantum state can be decomposed according to

$$|\psi\rangle_t = \sum_{\mathbf{k},i} a_{g\mathbf{k}i}(t) e^{-i(E_g + \hbar\omega_{\mathbf{k}})t/\hbar} |g\rangle \otimes \hat{a}_{\mathbf{k},i}^\dagger |0\rangle + a_e(t) e^{-iE_e t/\hbar} |e\rangle \otimes |0\rangle. \quad (13)$$

The resulting dynamics is described by the time-dependent Schrödinger equation with Hamiltonian

$$\begin{aligned} \hat{H} = & E_g |g\rangle\langle g| + E_e |e\rangle\langle e| + \sum_{\mathbf{k} \in I, i} \hbar\omega_{\mathbf{k}} \hat{a}_{\mathbf{k},i}^\dagger \hat{a}_{\mathbf{k},i} \\ & - |e\rangle\langle g| \langle e|\hat{\mathbf{d}}|g\rangle \cdot \hat{\mathbf{E}}_+(\mathbf{x}_0) - |g\rangle\langle e| \langle e|\hat{\mathbf{d}}|g\rangle^* \cdot \hat{\mathbf{E}}_-(\mathbf{x}_0) \end{aligned} \quad (14)$$

in the dipole- and rotating wave approximation [28]. The rotating wave approximation takes into account the interaction of the two-level system with the almost resonant field modes ( $\mathbf{k} \in I$ ) within a frequency interval of width  $\Delta\omega \gg \Gamma$  centered around the transition frequency  $\omega_{eg}$  in a non-perturbative way. The influence of all other (nonresonant) field modes can be taken into account perturbatively. In particular, in second-order perturbation theory these nonresonant modes give rise to a Lamb shift [30, 31]. It should be mentioned that, contrary to the almost resonant modes, for a consistent treatment of this energy shift the coupling of the nonresonant modes of the radiation field to the two-level atom cannot be treated in the dipole approximation because also high-frequency field modes have to be taken into account. Furthermore, mass renormalization has to be included. This way a well-defined and finite expression for the Lamb shift can even be obtained within a nonrelativistic quantum electrodynamical description [31].

The time-dependent Schrödinger equation is equivalent to the differential equations

$$\begin{aligned} \dot{a}_e(t) &= -\frac{\langle e|\hat{\mathbf{d}}|g\rangle}{\hbar} \sum_{\mathbf{k} \in I, i} \sqrt{\frac{\hbar\omega_{\mathbf{k}}}{2\epsilon_0}} \mathbf{u}_{\mathbf{k},i}(\mathbf{x}_0) a_{g\mathbf{k}i}(t) e^{i(E_e - E_g - \hbar\omega_{\mathbf{k}})t/\hbar}, \\ \dot{a}_{g\mathbf{k}i}(t) &= \frac{\langle e|\hat{\mathbf{d}}|g\rangle^*}{\hbar} \sqrt{\frac{\hbar\omega_{\mathbf{k}}}{2\epsilon_0}} \mathbf{u}_{\mathbf{k},i}^*(\mathbf{x}_0) a_e(t) e^{-i(E_e - E_g - \hbar\omega_{\mathbf{k}})t/\hbar} \end{aligned} \quad (15)$$



01 for the probability amplitudes which yield the integro-differential equation

$$02$$

$$03 \quad a_e(t) = - \sum_{\mathbf{k} \in I, i} \frac{\hbar \omega_{\mathbf{k}} |\langle e | \hat{\mathbf{d}} | g \rangle \cdot \mathbf{u}_{\mathbf{k}, i}(\mathbf{x}_0)|^2}{2 \hbar^2 \epsilon_0} \int_0^t dt' a_e(t') e^{i(E_e - E_g - \hbar \omega_{\mathbf{k}})(t-t')/\hbar} \quad (16)$$

06 for the probability amplitude  $a_e(t)$  of observing the two-level system in its  
 07 excited state  $|e\rangle$  at time  $t > 0$ . In the continuum limit of a large quantization  
 08 volume  $V$  the summation over the modes of the electromagnetic field can be  
 09 approximated by

$$11 \quad \sum_{\mathbf{k} \in I, i} \rightarrow \sum_i \frac{V}{(2\pi)^3} \int_{\mathbf{k} \in I} d^3 \mathbf{k} = \sum_i \int_{\omega \in I} d\omega \rho(\omega), \quad (17)$$

15 with  $\rho(\omega) = 4\pi V \omega^2 / (8\pi^3 c^3)$  enumerating the number of field modes per fre-  
 16 quency and per polarization. As long as the spontaneous decay rate  $\Gamma$  of  
 17 Eq. (12) is much smaller than the resonance frequency  $\omega_{eg}$  and the frequency  
 18 range over which the integrand of Eq. (16) varies significantly, the ‘‘pole  
 19 approximation’’ [7, 8, 32] may be applied so that Eq. (16) reduces to

$$21 \quad a_e(t) = - \int_0^t dt' \Gamma a_e(t') \delta(t - t') = -\frac{\Gamma}{2} a_e(t). \quad (18)$$

24 Within this approximation the initially excited two-level atom decays expo-  
 25 nentially with rate (12) so that for  $t > 0$  the quantum state is given by

$$27 \quad |\psi\rangle_t = \sum_{\mathbf{k} \in I, i} (-i) \langle e | \hat{\mathbf{d}} | g \rangle^* \cdot \mathbf{u}_{\mathbf{k}, i}^*(\mathbf{x}_0) \sqrt{\frac{\hbar \omega_{\mathbf{k}}}{2 \epsilon_0}} \frac{e^{-i(E_g + \hbar \omega_{\mathbf{k}})t/\hbar} - e^{-i(E_e - i\hbar\Gamma/2)t/\hbar}}{E_e - E_g - \hbar \omega_{\mathbf{k}} - i\hbar\Gamma/2} \hat{a}_{\mathbf{k}, i}^\dagger |0\rangle \otimes |g\rangle$$

$$30 \quad + e^{-i(E_e - i\hbar\Gamma/2)t/\hbar} |e\rangle \otimes |0\rangle. \quad (19)$$

32 Thus, at the end of the spontaneous decay process the two-level system  
 33 approaches a separable pure quantum state with the two-level system in  
 34 its lower energy eigenstate  $|g\rangle$ . In this quantum state the mean electric and  
 35 magnetic field strengths vanish so that the (normally ordered) energy den-  
 36 sity of the electromagnetic field provides a local measure for the statistical  
 37 uncertainty of these electromagnetic field strengths.

38 According to Eq. (19) after the completion of the photon emission process  
 39 both the two-level system and the electromagnetic field are in pure states.  
 40 In view of this asymptotic separation it is of interest to ask whether a one-  
 41 photon state of the electromagnetic field exists which is capable of exciting  
 42 a material system, such as an atom, perfectly in free space from an ini-  
 43 tially prepared ground state  $|g\rangle$  to an excited state  $|e\rangle$  by photon absorption.  
 44 Within our quantum electrodynamical model this question can be answered

in the affirmative in a straightforward way. For this purpose one has to solve Eqs. (15) subject to the final state condition that at a particular time, say  $t = 0$ , the two-level system is in its excited state and the radiation field in its vacuum state. It is straightforward to show that for  $t \leq 0$  this advanced solution of Eqs. (15) is given by the quantum state

$$|\psi\rangle_t = \sum_{\mathbf{k} \in I, i} (-i) \langle e | \hat{\mathbf{d}} | g \rangle^* \cdot \mathbf{u}_{\mathbf{k}, i}^*(\mathbf{x}_0) \sqrt{\frac{\hbar \omega_{\mathbf{k}}}{2\epsilon_0}} \frac{e^{-i(E_g + \hbar \omega_{\mathbf{k}})t/\hbar} - e^{-i(E_e + i\hbar\Gamma/2)t/\hbar}}{E_e - E_g - \hbar \omega_{\mathbf{k}} + i\hbar\Gamma/2} \hat{a}_{\mathbf{k}, i}^+ |0\rangle \otimes |g\rangle + e^{-i(E_e + i\hbar\Gamma/2)t/\hbar} |e\rangle \otimes |0\rangle. \quad (20)$$

Indeed, for  $t \rightarrow -\infty$  this quantum state is separable. It describes the two-level system initially prepared in state  $|g\rangle$  with the radiation field prepared in the particular pure one-photon state which finally excites the two-level system to its excited state  $|e\rangle$  perfectly by absorption of a single photon. For times  $t > 0$  the continuation of this time evolution is described by the quantum state of Eq. (19).

### 3. QUANTUM ELECTRODYNAMICS WITH CONTROLLED MODE SELECTION

In this section characteristic quantum phenomena originating from the exchange of energy between a two-level system and a single-photon radiation field inside a cavity are discussed. First, we consider a possibly large but closed spherical cavity which may contain many almost resonant field modes coupling to a material two-level system positioned in the center of the cavity. By varying the size of this cavity it is possible to describe in a uniform way the transition between the extreme cases of coupling to a single mode of the radiation field and of the free-space limit [23, 33]. Second, we discuss the dynamics of spontaneous photon emission by a two-level system in a half-open parabolic cavity.

#### 3.1. Photon exchange in a closed spherical cavity

The dynamics of a material two-level system positioned at the center  $\mathbf{x}_0$  of a spherical cavity, which supports almost resonant field modes, can be described within the theoretical framework discussed in Section 2.2. In the dipole- and rotating wave approximation again the dynamics of this quantum system can be described by the Hamiltonian of Eq. (14) in the Schrödinger picture. However, now the electric field operator of Eq. (10) has to be constructed with the help of mode functions  $\mathbf{u}_l(\mathbf{x})$  which are appropriate for a spherical cavity. For this purpose we solve the Helmholtz equation (4) with the boundary condition of an ideal metallic spherical cavity. Thus, the tangential component of  $\mathbf{u}_l(\mathbf{x})$  and the normal component of  $(\nabla \wedge \mathbf{u}_l)(\mathbf{x})$

01 have to vanish at the boundary of the spherical cavity. The corresponding  
02 solutions of the Helmholtz equation determine the relevant set of possible  
03 discrete eigenfrequencies  $\omega_l$  inside this cavity. For a spherical cavity of radius  
04  $R$  the possible mode functions are of the form [33]

$$\begin{aligned} 05 \quad \mathbf{U}_{nLM}(\mathbf{x}) &= N_{nL} j_L(\omega_{nL} r/c) \mathbf{X}_{LM}((\mathbf{x} - \mathbf{x}_0)/|\mathbf{x} - \mathbf{x}_0|), \\ 06 \quad \mathbf{V}_{nLM}(\mathbf{x}) &= N_{nL} \frac{ic}{\omega_{nL}} (\nabla \wedge j_L)(\omega_{nL} r/c) \mathbf{X}_{LM}((\mathbf{x} - \mathbf{x}_0)/|\mathbf{x} - \mathbf{x}_0|), \end{aligned} \quad (21)$$

07 with the mode index  $l \equiv (nLM)$ , the vector spherical harmonics [34]

$$08 \quad \mathbf{X}_{LM}(\mathbf{y}/|\mathbf{y}|) = -\frac{i}{\sqrt{L(L+1)}} \mathbf{y} \wedge (\nabla Y_L^M)(\mathbf{y}/|\mathbf{y}|), \quad (22)$$

09 and with the spherical harmonics  $Y_L^M(\mathbf{y}/|\mathbf{y}|)$  ( $L \in \mathbb{N}_0, -L \leq M \in \mathbb{Z} \leq L$ )  
10 [35]. The dependence of these mode functions on the radial coordinate  $r =$   
11  $|\mathbf{x} - \mathbf{x}_0|$  is determined by the regular spherical Bessel functions [35] whose  
12 asymptotic behavior is given by

$$13 \quad \frac{x^L}{(2L+1)!!} \overset{x \ll 1}{\leftarrow} j_L(x) \overset{x \gg 1}{\rightarrow} \frac{\sin(x - L\pi/2)}{x}, \quad (23)$$

14 with  $(2L+1)!! = (2L+1)(2L-1)(2L-3) \cdots 3 \cdot 1$ . The normalization constants  
15  $N_{nL}$  are given by

$$16 \quad N_{nL} = \left( \int_0^R dr r^2 j_L^2(\omega_{nL} r/c) \right)^{-1/2} \overset{n \gg 1}{\rightarrow} \frac{\omega_{nL}}{c} \sqrt{\frac{2}{R}}. \quad (24)$$

17 The eigenvalues  $\omega_{nL}$  of the electromagnetic field modes are determined by  
18 the metallic boundary conditions, i.e.,

$$19 \quad j_L(\omega_{nL} R/c) = 0, \quad \frac{d(x j_L(x))}{dx} \Big|_{x=\omega_{nL} R/c} = 0. \quad (25)$$

20 Thus, highly excited field modes with  $\omega_{nL} R/c \gg 1$  are characterized by the  
21 eigenvalues

$$22 \quad \omega_{nL} R/c \overset{\omega_{nL} R/c \gg 1}{\rightarrow} \pi n + (L+1)\pi/2. \quad (26)$$

23 Note that the energy density of highly excited field modes is given by  
24  $dn/d(\hbar\omega_{nL}) = R/(\pi\hbar c)$  and is thus frequency independent. It should also be  
25 mentioned that at the center of the spherical cavity, i.e., at  $\mathbf{x}_0$ , only the mode

01 functions  $\mathbf{V}_{nL=1M=0}(\mathbf{x})$  are nonvanishing. Therefore, in the dipole approxima-  
 02 tion the two-level system positioned at the center of the spherical cavity can  
 03 only couple to these field modes.

04 Inserting the relevant mode functions into the electric field operator of  
 05 Eq. (10) and solving the time-dependent Schrödinger equation with Hamil-  
 06 tonian (14) yields the time evolution of the quantum state  $|\psi\rangle_t$  [23]. As a  
 07 result, under the condition  $|\psi\rangle_{t=0} = |e\rangle \otimes |0\rangle$  in the limit of an infinitely  
 08 large cavity again the results of Eqs. (19 and 20) are obtained. In particu-  
 09 lar, with the help of the relevant mode functions  $\mathbf{V}_{nL=1M=0}(\mathbf{x})$  the energy  
 10 distribution of the resulting one-photon state can be determined in a straight-  
 11 forward way. In the radiation zone of the two-level system, i.e., at distances  
 12  $|\mathbf{x} - \mathbf{x}_0| = r \gg c/\omega_{eg}$ , one can use the asymptotic form of the relevant spheri-  
 13 cal Bessel functions. Thus, for the quantum state of Eqs. (19 and 20) in this  
 14 region of space the energy density of the radiation field is well approxi-  
 15 mated by

$$16 \quad {}_t\langle\psi| : \frac{\epsilon_0}{2} (\hat{\mathbf{E}}^2(\mathbf{x}) + c^2 \hat{\mathbf{B}}^2(\mathbf{x})) : |\psi\rangle_t = \frac{3\Gamma\hbar\omega_{eg}}{8\pi c} \frac{\sin^2\theta}{r^2} e^{-\Gamma(|t|-r/c)} \Theta(|t| - r/c). \quad (27)$$

17  
 18  
 19  
 20 Thereby,  $::$  denotes the normal ordering [28] of the field operators,  $\theta$  is the  
 21 angle between the dipole moment  $\langle e|\hat{\mathbf{d}}|g\rangle$  and the direction of observation  
 22  $(\mathbf{x} - \mathbf{x}_0)$ , and  $\Theta(x)$  denotes the Heaviside unit-step function with  $\Theta(x) = 1$  for  
 23  $x \geq 0$  and zero elsewhere. The electromagnetic energy density of Eq. (27)  
 24 is a local measure for the uncertainties of the electric and magnetic field  
 25 strengths. It is apparent that this energy density has an exponential shape  
 26 with a spatial extension of the order of  $c/\Gamma$  and with a sudden decrease at  
 27 distance  $|\mathbf{x} - \mathbf{x}_0| = r = c|t|$  from the two-level system. Due to energy conser-  
 28 vation the total field energy contained in this one-photon wave packet equals  
 29  $\hbar\omega_{eg}(1 - e^{-\Gamma|t|})$ . The mean field energy density can also be decomposed into  
 30 its electric and magnetic contributions (which are equal) and into its various  
 31 polarization components. Thus, along direction  $\mathbf{e}$  the polarization compo-  
 32 nent of the mean electric energy density, for example, can be represented in  
 33 the form

$$34 \quad {}_t\langle\psi| : \frac{\epsilon_0}{2} (\mathbf{e} \cdot \hat{\mathbf{E}}(\mathbf{x}))^2 : |\psi\rangle_t = |\mathbf{e} \cdot \mathcal{E}(\mathbf{x}, t)|^2, \quad (28)$$

35  
 36 with the complex-valued electric one-photon energy-density amplitude

$$37 \quad \mathcal{E}(\mathbf{x}, t) = -i\sqrt{\frac{3\Gamma\hbar\omega_{eg}}{16\pi c}} \Theta(|t| - r/c) e^{i\text{sgn}(t)\omega_{eg}(|t|-r/c)} e^{-\Gamma(|t|-r/c)/2} \frac{\sin\theta}{r} \mathbf{e}_\theta \quad (29)$$

38  
 39 and with  $\text{sgn}(t)$  denoting the sign of  $t$ . Equation (29) is valid in the radi-  
 40 ation zone, i.e., for  $\omega_{eg}r/c \gg 1$ , as long as  $\omega_{eg} \gg \Gamma/2$  (compare with  
 41  
 42  
 43  
 44

01 Eq. (18) and the validity of the pole approximation). It demonstrates that  
 02 in the radiation zone the electromagnetic field energy is concentrated com-  
 03 pletely in the polarization direction  $\mathbf{e}_\theta$ . Integrating Eq. (28) over all space  
 04 (thereby neglecting contributions outside the radiation zone) the electric field  
 05 energy at time  $t$  is given by

$$06 \int_{\mathbb{R}^3} d^3\mathbf{x} |\mathcal{E}(\mathbf{x},t)|^2 = \frac{\hbar\omega_{eg}}{2}(1 - e^{-\Gamma|t|}). \quad (30)$$

07  
 08  
 09 The analogous expression for the magnetic one-photon energy-density  
 10 amplitude can be obtained from Eq. (29) by the replacement  $\mathbf{e}_\theta \rightarrow \mathbf{e}_\varphi$ . Thus,  
 11 the magnetic energy density is concentrated completely in the direction  $\mathbf{e}_\varphi$   
 12 and its integrated field energy contribution is also given by Eq. (30).

13 For finite values of the radius of the spherical cavity  $R$  the dynamics of  
 14 the photon exchange with the two-level system changes significantly. In the  
 15 extreme limit of a small cavity in which only one cavity mode is in resonance  
 16 with the spontaneously decaying two-level system the dynamics reduces to  
 17 the results of the Jaynes–Cummings–Paul model discussed previously. In  
 18 cases in which this resonant field mode is highly excited this single-mode  
 19 limit is realized if  $\Gamma dn/d(\omega_{nL=1}) = \Gamma R/(\pi c) \ll 1$  so that the cavity is small in  
 20 comparison with the extension of a one-photon wave packet which is gener-  
 21 ated by spontaneous emission in free space and whose spatial extension  
 22 would be of the order of  $c/\Gamma$ . For larger values of the cavity radius  $R$  the  
 23 two-level system starts to couple to more and more field modes almost reso-  
 24 nantly so that eventually in the infinite cavity limit the free-field dynamics  
 25 is approached. It can be shown that for almost resonant coupling of the two-  
 26 level system to highly excited modes of the spherical cavity, i.e.,  $\omega_{eg}R/c \gg 1$ ,  
 27 for  $t \geq 0$  the time evolution of the excited-state probability amplitude for an  
 28 initially excited two-level system is given by

$$29 \langle e | \otimes \langle 0 | \psi \rangle_t = e^{-i(E_e - i\hbar\Gamma/2)t/\hbar} + \sum_{M=1}^{\infty} \Theta(t - 2MR/c) e^{-i(E_e - i\hbar\Gamma/2)(t - 2MR/c)/\hbar}$$

$$30 \times \left\{ \sum_{r=0}^{M-1} \binom{M-1}{r} \frac{[-\Gamma(t - 2MR/c)]^{1+r}}{(1+r)!} \right\}. \quad (31)$$

31  
 32  
 33 In Figure 8.2 this time evolution is depicted for various sizes of the spherical  
 34 cavity. For small cavities the characteristic almost periodic energy exchange  
 35 between the two-level system and the radiation field is apparent. For larger  
 36 cavity sizes this dynamics is modified. For large cavities with  $\Gamma dn/d(\omega_{nL=1}) =$   
 37  $\Gamma R/(\pi c) \gg 1$  the initially excited two-level system decays approximately  
 38 exponentially with rate  $\Gamma$  and is excited again at later times by the sponta-  
 39 neously generated one-photon wave packet whenever it returns again to the  
 40 center of the cavity where the two-level system is located.  
 41  
 42  
 43  
 44

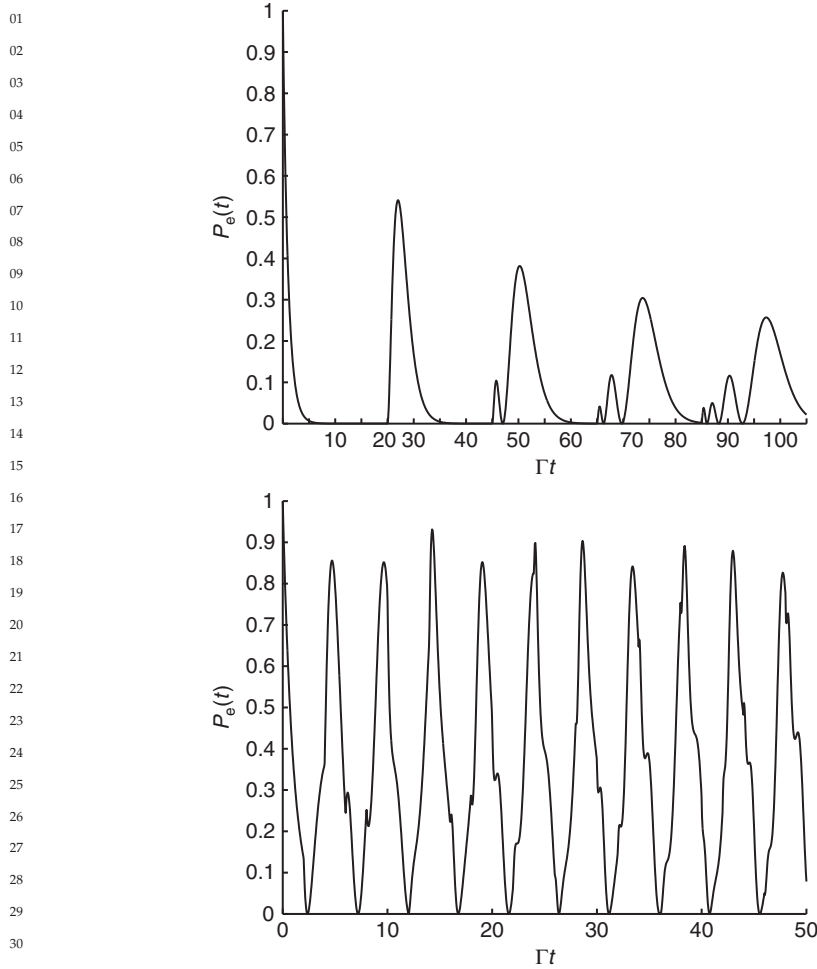


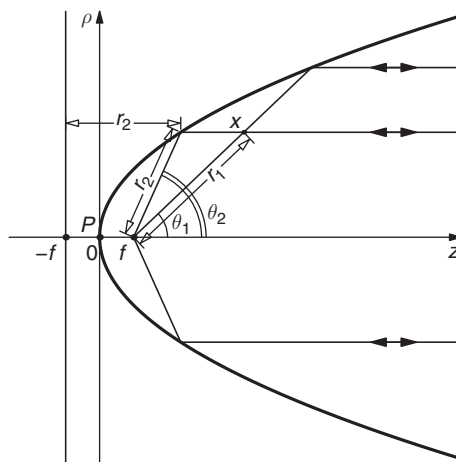
**Figure 8.2** Time dependence of the probability  $P_e(t)$  of observing the spontaneously decaying two-level system in its excited state at the center of a closed spherical cavity: The number of resonantly interacting field modes is of the order of  $\Gamma R/c$  and depends on the size of the cavity  $R$ . For  $\Gamma R/c = 10$  (left figure) a spatially localized photon wave packet is generated by spontaneous emission and can be reabsorbed again by the two-level system at the center of the cavity at later times. For  $\Gamma R/c = 1$  (right figure) only a small number of cavity modes interact resonantly and the two-level system performs approximate Rabi oscillations governed by the vacuum Rabi frequency.

### 3.2. Spontaneous photon emission in a half-open parabolic cavity

Efficient atom–light interaction in free space [20,36–38] may provide us with less technologically demanding solutions for quantum communication over large distances than typical cavity quantum electrodynamical solutions [13].

01 Thus, it has gained a lot of interest recently. An intermediate case between  
 02 the small-cavity limit and the free-space limit can be realized by a large  
 03 closed cavity [23] in which an atom couples to a large number of modes  
 04 and which has been discussed in the previous section. A half-cavity, i.e.,  
 05 a cavity with one mirror, constitutes another example of such a case. The  
 06 structure of standing light waves in front of a mirror was already analyzed  
 07 in the pioneering work of K. Drexhage [39]. Later on, it has been verified  
 08 experimentally that under such circumstances one can witness a change of  
 09 the density of states of the electromagnetic field modes near the atom by  
 10 measuring its spontaneous emission rate [40]. A simplified one-dimensional  
 11 scalar model of a laser-driven atom in a half-cavity has been discussed in  
 12 Ref. [41], for example.

13 As a second example for modifications of the quantum electrodynamical  
 14 interaction between matter and the radiation field originating from controlled  
 15 mode engineering in the following we discuss the spontaneous decay  
 16 of a two-level system, such as an ion [24], in a half-open cavity with a  
 17 parabolic shape. The two-level system is assumed to be positioned in the  
 18 focus  $F$  of an axially symmetric parabola whose boundary is formed by an  
 19 ideal metal and is described by the equation  $z = \rho^2/(4f)$  (compare with  
 20 Figure 8.3). The coordinate  $z$  measures distances from point  $P$  along the



21  
22  
23  
24  
25  
26  
27  
28  
29  
30  
31  
32  
33  
34  
35  
36  
37 **Figure 8.3** Spontaneous photon emission in a parabolic cavity: The two-level system  
 38 is positioned in the focus  $F$  of a metallic parabola with focal length  $f$ . All light rays emanating  
 39 from  $F$  which are reflected at the parabolic boundary leave the cavity by propagating parallel  
 40 to the symmetry axis. They all accumulate the same phase (eikonal) of magnitude  
 41  $\omega_{\text{eg}}(z+f)/c$  which is the same as if these light rays had started in phase from the plane  
 42  $z = -f$ . There are always two possible trajectories to any point  $\mathbf{x}$  inside the cavity. In the  
 43 semiclassical limit, i.e.,  $f \gg c/\omega_{\text{eg}}$ , these two classes of trajectories give rise to the  
 44 spherical-wave and the plane-wave contributions to the complex-valued energy-density  
 amplitude of Eq. (32).

01 symmetry axis and  $\rho$  denotes distances perpendicular to the symmetry axis.  
 02 The focal point  $F$  of the parabola has coordinates  $(z = f, \rho = 0)$  with  $f > 0$   
 03 denoting the focal length. A defining property of any parabola is the fact that  
 04 the distance between any point on its surface and the focal point  $F$  equals the  
 05 distance to the plane perpendicular to the symmetry axis located at  $z = -f$ .

06 We are particularly interested in possible changes of the spontaneous photon  
 07 emission process of a two-level system resulting from the presence of the  
 08 parabolic boundary conditions. The parabolic shape of the mirror ensures  
 09 that, if a light beam is sent parallel to the symmetry axis of the parabola  
 10 toward the two-level system, this two-level system interacts with the light  
 11 coming from the whole  $4\pi$  solid angle. Similarly, the whole light resulting  
 12 from spontaneous decay of the two-level system is redirected into a beam  
 13 propagating parallel to the symmetry axis. Thinking in terms of a semiclassical  
 14 ray picture only light rays which are emitted from the two-level system  
 15 along the (negative part of the) symmetry axis return again to the two-level  
 16 system. Contrary to the closed spherical cavity discussed in the previous  
 17 section all other emitted light rays leave the cavity without any reexcitation  
 18 of the two-level system. Thus, if the dipole moment of the two-level  
 19 system is oriented along the symmetry axis photon emission along the sym-  
 20 metry axis is suppressed and we do not expect any significant modification  
 21 of the spontaneous decay process of the two-level system due to the pres-  
 22 ence of the cavity in cases in which the focal length  $f$  is large in comparison  
 23 with the wavelength of a spontaneously emitted photon [42]. Nevertheless,  
 24 in analogy to a small cavity or to spontaneous emission in front of a planar  
 25 mirror [43] significant changes of the spontaneous decay rate are expected  
 26 if  $f$  becomes comparable to the wavelength of a spontaneously emitted  
 27 photon.

### 28 3.2.1. Time evolution of a photon wave packet

29 First of all, let us consider the dynamics of an almost resonant photon  
 30 and its resonant energy exchange with a two-level system positioned in  
 31 the focal point  $F$  in the semiclassical limit in which the focal length of  
 32 the parabola is large in comparison with the photon's wavelength, i.e.,  
 33  $f \gg c/\omega_{\text{eg}}$ . Furthermore let us concentrate on cases in which the two-level  
 34 system's dipole moment  $\langle e|\hat{\mathbf{d}}|g\rangle$  is oriented parallel to the symmetry axis  
 35 of the parabola. In particular, we want to investigate solutions of the time-  
 36 dependent Schrödinger equation  $|\psi\rangle_t$  for which at a certain instant of time,  
 37 say  $t = 0$ , the two-level system is excited and the electromagnetic radiation  
 38 field is in its vacuum state, i.e.,  $|\psi\rangle_{t=0} = |e\rangle \otimes |0\rangle$ . Thus, this case describes  
 39 spontaneous emission of a photon for  $t > 0$  and perfect excitation of the  
 40 two-level system by a one-photon field for  $t < 0$ . As  $f \gg c/\omega_{\text{eg}}$ , in the radi-  
 41 ation zone, i.e., for  $\omega_{\text{eg}}|\mathbf{x} - \mathbf{x}_0|/c \gg 1$ , the distribution of the energy density  
 42 of the electromagnetic field can be determined with the help of semiclas-  
 43 sical methods. This is due to the fact that the one-photon energy-density  
 44



01 amplitudes of the electric and magnetic field energies (compare with Eq. (29))  
 02 are rapidly oscillating functions of the radial variable  $r = |\mathbf{x} - \mathbf{x}_0|$  with a  
 03 slowly varying envelope which decays on the length scale  $c/\Gamma$ . Stated dif-  
 04 ferently, the condition  $\omega_{\text{eg}} \gg \Gamma/2$  implies that the phase (eikonal) of these  
 05 amplitudes exhibits many oscillations within the region of support of these  
 06 amplitudes.

07 In the radiation zone the one-photon energy-density amplitudes are solu-  
 08 tions of the wave equation whose semiclassical solutions [44] can be con-  
 09 structed with the help of the classical light rays inside the parabolic cavity.  
 10 Thus, the general form of the energy-density amplitudes of the electric and  
 11 magnetic field can be constructed semiclassically in two steps. First, one  
 12 determines their form inside a sphere of radius  $R_0$  around the focal point  
 13  $F \equiv \mathbf{x}_0$  so that the condition  $c/\omega_{\text{eg}} \ll R_0 \ll f$  is fulfilled. For the electric  
 14 field this amplitude is given by Eq. (29) and for the magnetic field it can  
 15 be obtained from Eq. (29) by the replacement  $\mathbf{e}_\theta \rightarrow \mathbf{e}_\varphi$ . Semiclassically,  
 16 with this form of these amplitudes one can associate a Lagrangian mani-  
 17 fold [44, 45] of radially outgoing straight-line trajectories which start at the  
 18 position of the two-level system  $F$  and which propagate with the speed of  
 19 light. The relevant polarization direction remains constant during transport  
 20 along these radial trajectories. In a second step one determines the most gen-  
 21 eral semiclassical solution of the wave equation within the parabolic cavity  
 22 but outside this sphere of radius  $R_0$ . For this purpose one has to construct  
 23 the light rays outside this sphere thereby taking into account that they are  
 24 reflected at the boundary of the cavity according to the classical reflection  
 25 law (equal incoming and outgoing angles). Apart from the reflection process  
 26 where one has to take into account the boundary conditions of an ideal metal  
 27 the polarization directions remain constant during the propagation along  
 28 any of these classical trajectories. The geometry of the parabola implies that  
 29 after reflection at the metallic boundary the classical trajectories propagate  
 30 parallel to the symmetry axis. Matching the solutions inside the sphere of  
 31 radius  $R_0$  and outside the sphere in a smooth way one obtains the one-photon  
 32 energy-density amplitude of the electric field at any point  $\mathbf{x} \equiv (z, \rho)$  inside the  
 33 parabolic cavity. Whereas for times  $|t| < f/c$  this energy-density amplitude  
 34 is given by Eq. (29), for times  $t > f/c$  it is modified due to reflections of light  
 35 rays at the boundary of the parabolic cavity and assumes the form

$$\begin{aligned}
 \mathcal{E}(\mathbf{x}, t) = & \\
 & -i\sqrt{\frac{3\Gamma\hbar\omega_{\text{eg}}}{16\pi c}} \Theta(|t| - r_1(z, \rho)/c) e^{i\text{sgn}(t)\omega_{\text{eg}}(|t| - r_1(z, \rho)/c)} e^{-\Gamma(|t| - r_1(z, \rho)/c)/2} \frac{\sin(\theta_1(z, \rho))}{r_1(z, \rho)} \mathbf{e}_{\theta_1} \\
 & + -i\sqrt{\frac{3\Gamma\hbar\omega_{\text{eg}}}{16\pi c}} \Theta\left(|t| - \frac{z+f}{c}\right) e^{i\text{sgn}(t)\omega_{\text{eg}}(|t| - (z+f)/c)} e^{-\Gamma(|t| - (z+f)/c)/2} \frac{\sin(\theta_2(\rho))}{r_2(\rho)} \mathbf{e}_{\rho'}
 \end{aligned} \tag{32}$$

with

$$\begin{aligned} \sin(\theta_1(z, \rho)) &= \frac{\rho}{r_1(z, \rho)}, r_1(z, \rho) = \sqrt{(z-f)^2 + \rho^2} \\ \sin(\theta_2(\rho)) &= \frac{\rho}{r_2(\rho)}, r_2(\rho) = f \left( 1 + \frac{\rho^2}{4f^2} \right). \end{aligned}$$

Therefore, at a fixed time  $t$  the contribution at position  $\mathbf{x} \equiv (z, \rho)$  results from the interference of contributions originating from radially propagating direct light rays (first term on the r.h.s. of Eq. (32)) with the contributions from light rays reflected at the boundary of the cavity (second term on the r.h.s. of Eq. (32)). Whereas the first type of contributions gives rise to a slowly modulated spherical wave front emanating from the position of the two-level system at  $F \equiv \mathbf{x}_0$ , the reflected trajectories give rise to a (rapidly varying) plane wave propagating in the  $z$ -direction with a slowly varying amplitude. This plane wave is a consequence of the parabolic geometry of the cavity and the fact that for any point on the boundary of the cavity its distances from the focal point  $F$  and from the plane  $z = -f$  are equal. Therefore, all light rays emitted at any angle  $\theta_2$  at  $F$  and reflected at the boundary of the parabolic cavity accumulate the same phase (eikonal). This phase is the same as the one originating from a fictitious set of trajectories starting from the plane  $z = -f$  and propagating along the  $z$ -axis with the speed of light. For large focal lengths in the sense that  $2f \gg c/\Gamma$  the two contributions to the energy-density amplitude are well separated in space apart from small regions around the boundary of the parabolic cavity. As a consequence interferences between contributions of these two different types of classical trajectories disappear. Furthermore, for a fixed value of  $\rho$  the spherical-wave contribution to Eq. (32) becomes vanishingly small in comparison with the plane-wave contribution in the limit of large values of  $z$ . It is apparent from Eq. (32) that the polarization properties of the spherical-wave contribution are not changed by the cavity and are the same as in free space. However, the polarization features of the plane-wave contribution are significantly different. At any point  $\mathbf{x}$  its polarization is directed in the  $\mathbf{e}_\rho$  direction so that the vector field  $\mathcal{E}(\mathbf{x}, t)$  represents a vortex field with respect to its polarization properties. The singularity at the symmetry axis is suppressed by the fact that there is no coupling between the radiation field and the two-level system along this axis because the dipole moment of the two-level system is oriented in this direction. Finally, it should be mentioned that the (primitive) semiclassical expression of Eq. (32) breaks down at points close to the boundary of the parabolic cavity where transitional or uniform semiclassical approximations [44, 46] have to be employed.

### 3.2.2. Modifications of the spontaneous decay rate

In this section it will be demonstrated that depending on the characteristic parameters, namely the focal length  $f$ , the resonant wavelength

01  $\lambda = (2\pi)c/\omega_{eg}$ , and the orientation of the two-level system's dipole moment  
 02  $d = \langle |\hat{\mathbf{d}}|g \rangle$ , the spontaneous decay rate of the two-level system may differ  
 03 significantly from its free-space value as given by Eq. (12).

04 Since the two-level system is located in a half-open space we start by  
 05 expanding the electric field operator (10) in mode functions suitable for the  
 06 parabolic symmetry of the problem. Following the results of Ref. [47] we use  
 07 mode functions of the form

$$08 \mathbf{E}_{k,\ell,\mu}^\sigma(\mathbf{r}) = \frac{k}{(2\pi)^{3/2}} \int_{S^2} d\mathbf{n} e^{i\mathbf{k}\cdot\mathbf{r}} h_{\ell,\mu}(\mathbf{n}) \mathbf{e}^\sigma(\mathbf{n}). \quad (33)$$

09 Thereby,  $\mathbf{k} = k\mathbf{n}$  denotes the wavevector,  $\sigma = 1, 2$  enumerates the polar-  
 10 ization states, and parameters  $\ell = 0, \pm 1, \pm 2, \dots$  and  $\mu \in (-\infty, +\infty)$   
 11 are additional mode indices. The unit vector  $\mathbf{n}$  and the polarization vectors  
 12  $\mathbf{e}^1(\mathbf{n}), \mathbf{e}^2(\mathbf{n})$  constitute the orthonormal basis which ensures the transversality  
 13 condition  $\nabla \cdot \mathbf{E} = 0$ . In particular, we choose these directions in the following  
 14 form:

$$15 \mathbf{n} = (\sin \theta \cos \varphi, \sin \theta \sin \varphi, \cos \theta), \quad (34)$$

$$16 \mathbf{e}^1(\mathbf{n}) = (\sin \varphi, -\cos \varphi, 0), \quad (35)$$

$$17 \mathbf{e}^2(\mathbf{n}) = (\cos \theta \cos \varphi, \cos \theta \sin \varphi, -\sin \theta). \quad (36)$$

18 The functions  $h_{\ell,\mu}(\mathbf{n})$  are explicitly given by [47]

$$19 h_{\ell,\mu}(\theta, \varphi) = \chi_\mu(\theta) \frac{e^{i\ell\varphi}}{\sqrt{2\pi}}, \quad (37)$$

20 with

$$21 \chi_\mu(\theta) = \frac{\exp(-i\mu \ln[\tan \theta/2])}{\sqrt{2\pi} \sin \theta}. \quad (38)$$

22 One can easily check the orthogonality and completeness conditions:

$$23 \int_0^{2\pi} d\varphi \int_0^\pi d\theta \sin \theta h_{\ell,\mu}^*(\theta, \varphi) h_{\ell',\mu'}(\theta, \varphi) = \delta_{\ell\ell'} \delta(\mu - \mu'), \quad (39)$$

$$24 \sum_{\ell=-\infty}^{+\infty} \int_{-\infty}^{+\infty} d\mu h_{\ell,\mu}^*(\theta, \varphi) h_{\ell,\mu}(\theta', \varphi') = \delta(\varphi - \varphi') \frac{\delta(\theta - \theta')}{\sin \theta}. \quad (40)$$

25 Combining Eq. (33) with Eq. (39) one obtains the orthogonality of the mode  
 26 functions, i.e.,

$$27 \int d\mathbf{r} \mathbf{E}_{k,\ell,\mu}^{*\sigma}(\mathbf{r}) \cdot \mathbf{E}_{k',\ell',\mu'}^{\sigma'}(\mathbf{r}) = \delta(k - k') \delta(\mu - \mu') \delta_{\ell\ell'} \delta_{\sigma\sigma'}. \quad (41)$$

If a two-level atom is positioned at  $\mathbf{x}$  in free space with the transition dipole parallel to the  $z$ -axis, in the dipole approximation the resulting spontaneous decay rate is given by

$$\Gamma(\mathbf{x}) = \frac{1}{(2\pi)^2} \frac{d^2k^3}{2\hbar\epsilon_0} \sum_{\sigma,\ell} \int_{-\infty}^{+\infty} d\mu \int d\mathbf{n} \int d\mathbf{n}' f_k(\mathbf{n}, \mathbf{r}) f_k^*(\mathbf{n}', \mathbf{r}) \cdot e_z^\sigma(\mathbf{n}) e_z^\sigma(\mathbf{n}') h_{\ell,\mu}^*(\mathbf{n}, k) h_{\ell,\mu}(\mathbf{n}', k), \quad (42)$$

with  $k = \omega_{eg}/c$ . Furthermore, we defined  $f_k(\mathbf{n}, \mathbf{r}) = \exp(ik\mathbf{n}\cdot\mathbf{r})$ ,  $e_z^\sigma(\mathbf{n}) = \mathbf{e}^\sigma(\mathbf{n})\cdot\mathbf{e}_z$  and used the fact that the summation over  $\ell$  produces  $\delta(\varphi - \varphi')$  (see Eq. (40)). Therefore, the relevant directions  $\mathbf{n}$ ,  $\mathbf{n}'$  and the  $z$ -axis belong to the same plane which leads to the relation

$$\sum_{\sigma} e_z^\sigma(\mathbf{n}) e_z^\sigma(\mathbf{n}') = e_z^2(\mathbf{n}) e_z^2(\mathbf{n}') = \sin\theta \sin\theta'. \quad (43)$$

Taking into account that the integration over  $\mu$  yields another Dirac delta distribution  $\delta(\theta - \theta')$  we finally obtain

$$\Gamma(x, y, z) = \frac{1}{(2\pi)^2} \frac{d^2k^3}{2\hbar\epsilon_0} \int_0^{2\pi} d\varphi \int_0^\pi d\theta \sin^3\theta |f_k(x, y, z; \varphi, \theta)|^2, \quad (44)$$

with  $\mathbf{x} \equiv (x, y, z)$  and  $f_k(\mathbf{n}, \mathbf{r}) \equiv f_k(x, y, z; \varphi, \theta)$ . The relation  $|f_k(x, y, z; \varphi, \theta)| = 1$  implies that we recover again the free-space result of Eq. (12).

In the presence of a conducting parabolic mirror the mode functions of Eq. (33) should fulfill the appropriate boundary conditions of an ideal metal. However, it is very challenging to solve the Helmholtz equation under these boundary conditions and the transversality condition simultaneously. Contrary to Ref. [48], a simplified approximation may be obtained by keeping the transversality condition but relaxing the precise conditions on the mode functions on the surface of the parabolic mirror. The transversality condition relates the electric field to the geometry of the system and therefore contributes to some geometrical factor present in the decay rate formula. The boundary condition ensures a possible discreteness of the normal modes. As our physical system is large it is expected that slightly changing the boundary conditions of the parabolic cavity will not influence the decay rate significantly.

We start our approximate treatment by introducing parabolic coordinates  $(\xi, \eta, \varphi)$  which are related to Cartesian coordinates by

$$x = 2\sqrt{\xi\eta} \cos\varphi, \quad (45)$$

$$y = 2\sqrt{\xi\eta} \sin\varphi, \quad (46)$$

$$z = \xi - \eta. \quad (47)$$

01 The boundary of the parabolic mirror is described by the equation  $\eta = f$ . It  
 02 can be shown [47] that the important  $\eta$ -dependent part of the mode functions  
 03 possesses the following asymptotic behavior:

$$04 \quad F_{\ell,\mu}(k; \eta) \sim \frac{\cos \{ \mu \ln 2k\eta + k\eta - \alpha_{\ell,\mu} \}}{\sqrt{\eta}}, \quad (48)$$

05 with a phase  $\alpha_{\ell,\mu}$  whose explicit form is not important for our subsequent  
 06 discussion. Imposing the parabolic boundary condition on Eq. (48) at the  
 07 value  $\eta = f$  results in a discrete set of values for  $\mu_m$ . A simple choice for these  
 08 discrete values is

$$09 \quad kf - \alpha_{\ell,\mu} = 0, \mu_m \ln 2kf = m\pi, m = 1, 2, 3, \dots \quad (49)$$

10 This particular choice is consistent with the replacement of the continuous  
 11 set of modes of Eq. (38) by the discrete set

$$12 \quad \tilde{\chi}_m(\theta) = \frac{\sin \left( \frac{m\pi \ln [\tan \theta/2]}{\ln 2kf} \right)}{\sqrt{2\pi \ln 2kf} \sin \theta} \quad \text{for } \theta \in [\theta_0, \pi - \theta_0] \quad (50)$$

$$13 \quad = 0 \text{ otherwise}$$

14 such that

$$15 \quad \tan \frac{\theta_0}{2} = \frac{1}{2kf} = \frac{1}{4\pi} \frac{\lambda}{f}. \quad (51)$$

16 The limitation on the angle  $\theta$  results from the quantization condition (49)  
 17 and from the fact that at the boundary the normal modes have to vanish, i.e.,  
 18  $\tilde{\chi}_m(\theta_0) = 0$ . This ansatz modifies the formula for the decay rate because the  
 19 completeness condition is changed according to

$$20 \quad \sum_m \tilde{\chi}_m(\theta) \tilde{\chi}_m(\theta') = I_{[\theta_0, \pi - \theta_0]}(\theta) \frac{\delta(\theta - \theta')}{\sin \theta}, \quad (52)$$

21 with  $I_A$  denoting the indicator function of the set  $A$ . Therefore, the integration  
 22 over the angle  $\theta$  involved in Eq. (42) should be performed over the interval  
 23  $[\theta_0, \pi - \theta_0]$ . This leads to a correction of the order of  $(kf)^{-4}$  which, however, is  
 24 not relevant for present-day experiments. In currently planned experiments  
 25 [24] typical focal lengths and wavelengths are of the order of  $f = 2$  mm and  
 26  $\lambda = 250$  nm which amounts to a value of  $kf \simeq 10^4$  [20] so that  $\theta_0$  is small.  
 27 Therefore, we can replace  $\sin \theta$  by  $\theta$ . It is rather obvious that the same is true  
 28 for any reasonable choice of the boundary conditions because the smallness  
 29 of this correction is entirely due to the large value of  $kf$ .

Hence the only relevant modification of the spontaneous emission rate due to the presence of the parabolic mirror is the replacement of the plane traveling waves  $f_k(\mathbf{n}, \mathbf{r}) = e^{i\mathbf{k}\mathbf{n}\cdot\mathbf{r}}$  by the standing waves

$$f_k(\mathbf{n}, \mathbf{r}) = \sqrt{2} \sin(\mathbf{k}\mathbf{n} \cdot (\mathbf{r} - \mathbf{f})), \quad (53)$$

where the factor  $\sqrt{2}$  ensures the completeness condition. Equation (53) implies that the electric field for any mode of the form of Eq. (33) vanishes at the point  $P$  of the parabola. It leads to the following approximate expression for the spontaneous emission rate in the presence of a conducting parabolic mirror:

$$\tilde{\Gamma}(x, y, z) = \frac{1}{2\pi^2} \frac{d^2k^3}{2\hbar\epsilon_0} \int_0^{2\pi} d\varphi \int_0^\pi d\theta \sin^3\theta \sin^2\{k[(x \cos\varphi + y \sin\varphi) \sin\theta + (z + f) \cos\theta]\}. \quad (54)$$

If the two-level system is placed at a distance from the point  $P$  which is much larger than  $\lambda = (2\pi)c/\omega_{eg}$ , the interference factor  $\sin^2(\dots)$  is averaged to  $1/2$  and the standard free-space result of Eq. (12) is recovered.

If the two-level system is located at the symmetry axis of the parabola, i.e.,  $x = y = 0$ , the integral in Eq. (54) simplifies to

$$\tilde{\Gamma}(z) = \eta\Gamma, \quad (55)$$

with the correction  $\eta$  to the free-space decay rate  $\Gamma$  being given by

$$\eta = \left( 1 + 3 \frac{\cos(2k(z+f))}{4k^2(z+f)^2} - 3 \frac{\sin(2k(z+f))}{8k^3(z+f)^3} \right). \quad (56)$$

For a focal length  $f = 2$  mm this correction factor  $\eta$  is depicted in Figure 8.4. Its value at the focal point  $F$  becomes significant for small values of the wave vector  $k = c/\omega_{eg}$ . This corresponds to cases in which the two-level system is close to the mirror surface, i.e.,  $|z + f| < \lambda$ . However, for larger values of  $k$  the variations of  $\eta$  are shifted toward the mirror surface. Far away from the mirror  $\eta$  tends to unity so that the decay rate reduces to its free-space value. According to these results modifications of the spontaneous decay rate could be observable on a scale of 100 nm but only within a distance of the order of the wavelength from the mirror surface.

#### 4. CONCLUSIONS AND OUTLOOK

Despite significant recent advances in the area of cavity quantum electrodynamics concerning the control of photonic quantum states and their interaction with matter in cavities, the interaction of few-photon multimode quantum states with matter in free space is still largely unexplored. A detailed

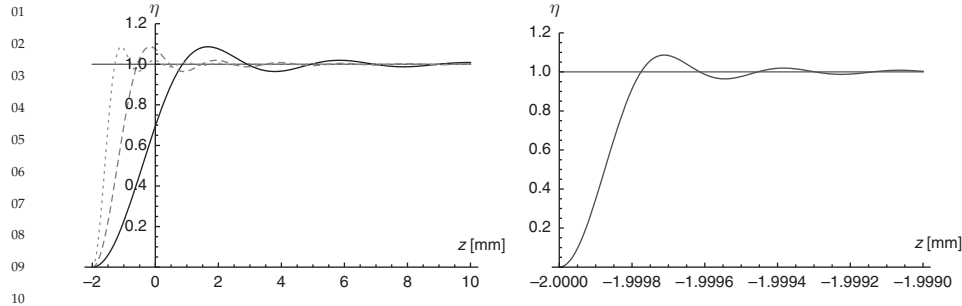


**Figure 8.4** Modifications of the spontaneous decay rate according to Eqs. (55 and 56): small values of  $k = (2\pi)c/\omega_{eg}$  (left figure):  $k = 0.25\pi \text{ mm}^{-1}$  – solid line,  $k = 0.5\pi \text{ mm}^{-1}$  – dashed line,  $k = \pi \text{ mm}^{-1}$  – dotted line; large value of  $k = 10^4 \text{ mm}^{-1}$  (right figure).

understanding of this interaction and the resulting exchange of quantum information between radiation field and matter is not only of general physical interest but also necessary for promising future quantum technological applications, such as the realization of quantum repeaters.

Here, we have discussed the simplest problem in this respect, namely the free-space interaction of a single-photon quantum state with an individual two-level matter system which can be realized by a trapped atom or ion. In this elementary example it can be demonstrated explicitly that the process of spontaneous emission of a photon is perfectly reversible provided that one is able to control the modes and quantum states of the radiation field in free space. For this purpose the dynamics resulting from the mode structure of a parabolic mirror has been discussed. It has been shown that using parabola it is possible to perfectly convert the excitation of an appropriately prepared asymptotically incoming plane-wave one-photon quantum state to an atom positioned in the focus of the parabola. The resulting dynamics depends strongly on the magnitudes of the dominantly excited wavelengths of the one-photon state. If these wavelengths are short in comparison with the focal length of the parabola the propagation of the one-photon state can be described by semiclassical methods and is dominated by the light rays of the photon inside the parabola. In the opposite limit of long wavelengths diffraction effects become important and semiclassical treatments become inappropriate.

Further experimental testing of the discussed theoretical results is planned. In our future experiment [24, 25] we will use a  $^{174}\text{Yb}^{2+}$  ion as a two-level system with  $^1S_0$  and  $^3P_1^0$  electronic levels as the ground and the excited states, respectively, and no hyperfine structure. The atomic transition frequency of 251.8 nm is in the ultraviolet regime. The ion will be trapped at the focus of a metallic parabolic mirror with focal length  $f = 2.1 \text{ mm}$  which forms one electrode of a Paul trap. The rf needle-shaped electrode will come



01 from the back of the mirror through a small hole. This trap design will ensure  
02 almost full  $4\pi$ -angle ion–light interaction in the strong focusing regime.  
03 The aberration corrections will be done using a diffractive element located  
04 in front of the mirror. The ion has only one decay channel and its dipole  
05 moment will be parallel to the mirror axis. There are several methods which  
06 allow for single-photon pulse generation with the desired spatiotemporal  
07 shape and spectral distribution. The first relies on electrooptic modulation of  
08 a single-photon wave packet [49]. Another experimentally more accessible  
09 method applies a strongly attenuated laser pulse containing  $\bar{n} \ll 1$  photons  
10 on average. This technique is widely used in quantum key distribution [50].  
11 We can shape the pulsed temporal mode structure electronically with mod-  
12 ulators starting from a continuous-wave laser. Next we will turn it into a  
13 radially polarized spatial doughnut mode. After reflection from the mirror  
14 surface its polarization at the focal point will only contribute to polarization  
15 parallel to the symmetry axis of the mirror and therefore will excite a lin-  
16 ear dipole oscillating parallel to this axis. Using this simpler method perfect  
17 coupling is achieved if the probability of excitation matches the probability  
18 of finding a single photon in the pulse. In addition, as a third option one can  
19 generate the properly shaped single-photon Fock state wave function condi-  
20 tionally using photon pairs from parametric downconversion. This method  
21 is similar to ghost imaging in the time domain.

22 Of course, none of these methods will produce an infinitely extended  
23 pulse. This is not an obstacle for our experiment however, because one can  
24 truncate somewhat the exponential tail of the one-photon wave packet. For  
25 example, truncating the pulse to a duration of five lifetimes the excitation  
26 probability can be as high as 0.99. For quantum storage applications it is  
27 straightforward to expand this scheme to a lambda transition between two  
28 long-lived states [51]. Furthermore, efficient coupling in free space opens the  
29 possibility for nonlinear optics at the single-photon level.

30 The investigations discussed here present first steps toward the future goal  
31 of obtaining a detailed understanding of the interaction of individual pho-  
32 tons with individual atoms in free space. For future applications in quantum  
33 information technology the exploration of the limits of perfect exchange of  
34 quantum information between the radiation field and these material systems  
35 is of particular interest.

## 37 REFERENCES

- 38  
39  
40 [1] W. Heisenberg, *Z. Phys.* 33 (1925) 879.  
41 [2] I.J.R. Aitchison, D.A. MacManus, Th.M.Snyder, Understanding Heisenberg's 'Magical'  
42 Paper of July 1925: A New Look at the Computational Details, arXiv:quant-ph/0404009.  
43 [3] M. Born, P. Jordan, *Z. Phys.* 34 (1925) 858.  
44 [4] E. Schrödinger, *Ann. Phys.* 79 (1926) 361; 79 (1926) 489.  
[5] E. Schrödinger, 79 (1926) 734.



- 01 [6] P.A.M. Dirac, Proc. R. Soc. A 109 (1926) 642.  
 02 [7] V. Weisskopf, E. Wigner, Z. Phys. 63 (1930) 54.  
 03 [8] V. Weisskopf, E. Wigner, Z. Phys. 65 (1930) 18.  
 04 [9] Th. Beth, G. Leuchs (Eds.), Quantum Information Processing, Wiley-VCH, Weinheim, 2005.  
 05 [10] D. Leibfried, R. Blatt, C. Monroe, D. Wineland, Rev. Mod. Phys. 75 (2003) 281.  
 06 [11] J. Fortagh, C. Zimmermann, Rev. Mod. Phys. 79 (2007) 235.  
 07 [12] C. Winterfeldt, Ch. Spielmann, G. Gerber, Rev. Mod. Phys. 80 (2008) 117.  
 08 [13] H. Walther, B.T.H. Varcoe, B.G. Englert, T. Becker, Rep. Prog. Phys. 69 (2006) 1325.  
 09 [14] E.A. Purcell, Phys. Rev. 69 (1946) 681 (Note B10).  
 10 [15] D. Kleppner, Phys. Rev. Lett. 47 (1981) 233.  
 11 [16] W.Jhe, A. Anderson, E.A. Hinds, D. Meschede, L. Moi, S. Haroche, Phys. Rev. Lett. 58  
 (1987) 666.  
 12 [17] B.T.H. Varcoe, S. Brattke, M. Weidinger, H. Walther, Nature 403 (2000) 743.  
 13 [18] W.P. Schleich, Quantum Optics in Phase Space, Wiley-VCH, Weinheim, 2001.  
 14 [19] S. Quabis, R. Dorn, M. Eberler, O. Glöckl, G. Leuchs, Opt. Commun. 179 (2000) 1.  
 15 [20] M. Stobińska, G. Alber, G. Leuchs, EPL 86 (2009) 14007.  
 16 [21] E.T. Jaynes, F.W. Cummings, Proc. IEEE 51 (1963) 89.  
 17 [22] H. Paul, Ann. Phys. 11 (1963) 411.  
 18 [23] G. Alber, Phys. Rev. A 46 (1992) R5338.  
 19 [24] M. Sondermann, R. Maiwald, H. Konermann, N. Lindlein, U. Peschel, G. Leuchs, Appl.  
 Phys. B, 89 (2007) 489.  
 20 [25] R. Maiwald, D. Leibfried, J. Britton, J.C. Bergquist, G. Leuchs, D.J. Wineland, Nat. Phys. 5  
 (2009) 551.  
 21 [26] J.H. Eberly, N.B. Narozhny, J.J. Sanchez-Mondragon, Phys. Rev. Lett. 44 (1980) 1323.  
 22 [27] I.Sh. Averbukh, N.F. Perel'man, Phys. Lett. A 139 (1989) 449.  
 23 [28] L. Mandel, E. Wolf, Optical Coherence and Quantum Optics, Cambridge University Press,  
 Cambridge, 1995.  
 24 [29] P. Goy, J.M. Raimond, M. Gross, S. Haroche, Phys. Rev. Lett. 50 (1983) 1903.  
 25 [30] H.A. Bethe, Phys. Rev. 72 (1947) 339.  
 26 [31] J. Seke, Nuovo Cimento D 18 (1996) 533.  
 27 [32] J. Seke, Phys. Lett. A 244 (1998) 111.  
 28 [33] G. Alber, G.M. Nikolopoulos, In: Lectures on Quantum Information, D. Bruss, G. Leuchs,  
 (Eds.), Wiley-VCH, Weinheim, 2007 p. 555ff.  
 29 [34] J.D. Jackson, Classical Electrodynamics, Wiley, New York, 1975.  
 30 [35] M. Abramowitz, I. Stegun (Eds.), Handbook of Mathematical Functions, National Bureau  
 of Standards Applied Mathematics Series No. 55, US. GPO, Washington, DC, 1964.  
 31 [36] I. Gerhardt, G. Wrigge, P. Bushev, G. Zumofen, M. Agio, R. Pfab, et al., Phys. Rev. Lett. 98,  
 32 (2007) 033601.  
 33 [37] G. Zumofen, N.M. Mojarad, V. Sandoghdar, M. Agio, Phys. Rev. Lett. 101, (2008) 180404.  
 34 [38] M.K. Tey, Z. Chen, S.A. Aljunid, B. Chng, F. Huber, G. Maslennikov, et al., Nat. Phys. 4  
 (2008) 924.  
 35 [39] K.H. Drexhage, Sci. Am. 222 (1970) 108.  
 36 [40] J. Eschner, Ch. Raab, R. Blatt, Nature 413 (2001) 495.  
 37 [41] U. Dörner, P. Zoller, Phys. Rev. A 66, (2002) 023816.  
 38 [42] M. Stobińska, R. Alicki, Single-Photon Single-Ion Interaction in Free Space Configuration  
 in Front of a Parabolic Mirror, arXiv:quant-ph/0905.4014.  
 39 [43] H. Morawitz, Phys. Rev. 187 (1969) 1792.  
 40 [44] V.P. Maslov, M.V. Fedoriuk, Semi-Classical Approximation in Quantum Mechanics, Reidel,  
 Dordrecht, 1981.  
 41 [45] V.I. Arnold, Mathematical Methods of Classical Mechanics, Springer, Berlin, 1978.  
 42 [46] M.V. Berry, K.E. Mount, Rep. Prog. Phys. 35 (1972) 315.  
 43 [47] C.P. Boyer, E.G. Kalnins, W. Miller, Nagoya Math. J. 60 (1976) 35.  
 44

- 01 [48] J.U. Nockel, G. Bourdon, E. Le Ru, R. Adams, I. Robert, J.-M. Moison, et al., Phys. Rev. E 62  
02 (2000) 8677.  
03 [49] P. Kolchin, C. Belthangady, S. Du, G. Y. Yin, S.E. Harris, Phys. Rev. Lett. 101 (2008) 103601.  
04 [50] N. Gisin, G. Ribordy, W. Tittel, H. Zbinden, Rev. Mod. Phys. 74 (2002) 145.  
05 [51] D. Pinotsi, A. Imamoglu, Phys. Rev. Lett. 100 (2008) 093603.  
06  
07  
08  
09  
10  
11  
12  
13  
14  
15  
16  
17  
18  
19  
20  
21  
22  
23  
24  
25  
26  
27  
28  
29  
30  
31  
32  
33  
34  
35  
36  
37  
38  
39  
40  
41  
42  
43  
44